International Journal of Thin Films Science and Technology

http://dx.doi.org/10.18576/ijtfst/070105

The Rod Eutectic Growth under Rapid Solidification Conditions

Xiao-Hua Xu and Ming-Wen Chen*

School of Mathematics and Physics, University of Science and Technology Beijing, Beijing 100083, China

Received: 12 Nov. 2017, Revised: 23 Dec. 2017, Accepted: 28 Dec. 2017.
Published online: 1 Jan. 2018.

Abstract: The Jackson–Hunt model of rod eutectic growth is extended from low velocities to high velocities in rapid solidification conditions. When the eutectic growth under rapid solidification conditions and the eutectic alloys contain the phases that have sluggish interface-attachment kinetics, the effect of interface kinetics on the eutectic growth is significant. The relation between the interface kinetics, growth velocity, rod spacing and interface undercooling can be derived. The results reveal that a small spacing and a large undercooling in the system require a large Peclet number p coupled with a small distribution coefficient k. The expressions $\lambda^2 V$ and $\lambda\Delta T$ are constants at low velocities, while variables at high velocities. The rod spacing decreases while the rod eutectic growth velocity increases as the kinetic parameter increases.

PACS: 81.10Aj, 61.50.Ah, 68.35Ja

Keywords: Rod eutectic; Arbitrary distribution coefficient; Interface kinetics; Large Peclet number.

1 Introduction

The rod eutectic is a kind of fundamental interfacial microstructure with periodic growth pattern [1]. The periodic growth pattern determines the mechanical and physical properties of the rod eutectic alloys. The extensive experimental and theoretical investigations on the periodic pattern characteristics and coupled growth behavior in solidification of the rod eutectic alloys have greatly enhanced the understanding of interfacial microstructure of the rod eutectic alloys [2-7]. Jackson and Hunt (JH) [7] presented a general theory for the growth of rod and lamellar eutectics, and revealed the relation between the interface undercooling ΔT at the solid-liquid interface and the eutectic spacing λ at low velocity V, namely $\Delta T = K_1 \lambda V + K_2 / \lambda$, where K_1 and K_2 are material constants. By using minimum undercooling principle, they obtained the well-known relation between λ and V, thus $\lambda^2 V = K_2 / K_1$. Trivedi, Magnin and Kurz [8] (TMK) investigated the characteristics of lamellar eutectic structures under rapid solidification conditions and found that the expression $\lambda^2 V$ is not a constant, but depends upon the Peclet number, $p = V\lambda / 2D$, where D is the diffusion coefficient of solute in the liquid. When the eutectic growth under rapid solidification conditions and the eutectic alloys contain the phases that have sluggish interface-attachment kinetics, the effect of interface kinetics on eutectic growth is significant [9-11]. Li and Zhou [12] studied the effect of the interface kinetics on the lamellar eutectic growth and found that if the effect of interface kinetics on the growth of the lamellar eutectic is taken into consideration, the coupled eutectic growth can proceed in a wider undercooling range. Li, Yoda and Kuribayashi [13] studied the effect of the asymmetrical contribution of kinetics on the eutectic growth. They found that it is the kinetic undercooling of the facetted or the non-facetted phases that enable the coupled eutectic composition to facetted phase so that to balance the kinetics contribution and weaken the solute undercooling of the facetted phase.

In this paper, based on two types of phase diagrams, we study the effect of interface kinetics on the rod eutectic growth under rapid solidification conditions. The first type of phase diagrams is the phase diagram in which the distribution coefficients are equal to each other, thus $k = k_\alpha = k_\beta$, where k is a constant, k_α and k_β denote the distribution coefficients of α and β phases, respectively. The second type of phase diagrams is the cigar-shaped phase diagram, in which the solidus and the liquidus lines are parallel when the temperature is below the eutectic temperature. Jackson-Hunt model of rod eutectic growth is extended from low velocities to high velocities under rapid

*Corresponding author E-mail: chenmw@ustb.edu.cn

© 2018 NSP
Natural Sciences Publishing Cor.

solidification conditions. The approach we used is similar to that in the JH model, but we have considered the effects of diffusion coefficient on the solute concentration, the interface undercooling and the rod spacing, as well as the effects of interface kinetics on the rod spacing and the interface undercooling. We seek the analytical expressions of the solute concentration, $\lambda^2 V$ and the total undercooling included the effect of the kinetic undercooling, which then can reveal the growth mechanism of the rod eutectic under rapid solidification conditions.

2 The Mathematical Model

A typical rod eutectic structure is showed in **Fig.** 1(a), where a normal view to its interface is presented. We replace the polygonal boundary by a circle with radius $r = r_\alpha + r_\beta$. The rod phase is denoted as the α-phase with radius r_α and the inter-rod phase as the β-phase with radius r_β. The center of the rod in the plane of the interface is taken as the origin of the coordinate system, with r being the radial distance and z being the distance from the interface in the growth direction, as showed in **Fig.** 1(b). The solute concentration $C(r,z)$ satisfies the steady state diffusion equation

$$\frac{\partial^2 C}{\partial r^2}+\frac{1}{r}\frac{\partial C}{\partial r}+\frac{\partial^2 C}{\partial^2 z}+\frac{V}{D}\frac{\partial C}{\partial z}=0 \tag{1}$$

With the boundary conditions:

1. The far field condition: as $z\to\infty$,

$$C\to C_\infty . \tag{2}$$

2. The interface-tip' condition: at $r=0$ and at $r=r_\alpha+r_\beta$,

$$\partial C/\partial r = 0 . \tag{3}$$

3. The solute conservation condition

$$\frac{\partial C}{\partial z}\Big|_{z=0}=-\frac{(1-k_\alpha)V}{D}C(r,0),\quad 0\le r<r_\alpha , \tag{4}$$

$$\frac{\partial C}{\partial z}\Big|_{z=0}=\frac{(1-k_\beta)V}{D}[1-C(r,0)],\quad r_\alpha<r\le r_\alpha+r_\beta . \tag{5}$$

By using the method of separation of variables, we seek the solution for Eqs. (1)-(3). We assume that the general solution of Eq. (1) has the form $C=R(r)Z(z)+C_\infty$. Insert it into Eqs. (1)-(3) and derive the bounded solutions

$$R(r)=\sum_{n=0}^{\infty}a_n J_0\left(\frac{\gamma_n}{r_\alpha+r_\beta}r\right),\ Z(z)=b_n e^{-w_n z}, \tag{6}$$

where $J_0(x)$ is the Bessel function of order zero, a_n and b_n are unknown constants, γ_n are the roots of $J_1(x)=0$. And the function w_n is defined as

$$w_n=\frac{V}{2D}+\sqrt{\left(\frac{V}{2D}\right)^2+\left(\frac{\gamma_n}{r_\alpha+r_\beta}\right)^2} . \tag{7}$$

Then the concentration of the solute diffusion is expressed as

$$C=C_\infty+\sum_{n=0}^{\infty}A_n e^{-w_n z}J_0\left(\frac{\gamma_n r}{r_\alpha+r_\beta}\right), \tag{8}$$

Where A_n $(A_n=a_n b_n, n=1,2,\cdots)$ are unknown constants, which are determined by the solute conservation condition on the interface. By assuming that $w_n\approx\gamma_n/(r_\alpha+r_\beta)$ and the interface concentration $C(r,0)$ is approximately eutectic concentration C_e, i.e. $C(r,0)\approx C_e$, Jackson and Hunt [7] obtained the approximate concentration distribution at low velocities. However, at high velocities, these two assumptions are both no longer valid. Instead, w_n should be treated as Eq. (7), and the interface concentration depends implicitly on r, the distance far away from the center of the rod eutectic. For two types of phase diagrams, we want to determine the concentration distribution of the rod eutectic at high velocities.

2.1 The first Type: Arbitrary Constant Distribution Coefficient

When the distribution coefficient is an arbitrary constant which satisfies $k=k_\alpha=k_\beta$, the solute conservation condition at the interface is expressed as

$$\frac{\partial C}{\partial z}\Big|_{z=0}=-\frac{(1-k)V}{D}C(r,0),\quad 0\le r<r_\alpha , \tag{9}$$

$$\frac{\partial C}{\partial z}\Big|_{z=0}=\frac{(1-k)V}{D}[1-C(r,0)],\quad r_\alpha<r\le r_\alpha+r_\beta . \tag{10}$$

Using the concentration in (8) and inserting (8) into (9)-(10), we obtain the Bessel coefficients A_0 and A_n in Eq. (8)

$$A_0=\frac{1-k}{k}\left[C_\infty f-(1-C_\infty)(1-f)\right],$$

$$A_n=\frac{2(1-k)V(r_\alpha+r_\beta)}{\gamma_n^2 D}\frac{\sqrt{f}J_1(\sqrt{f}\gamma_n)}{(J_0(\gamma_n))^2}\left(\frac{P_n}{\sqrt{1+P_n^2}-1+2k}\right), \tag{11}$$

© 2018 NSP
Natural Sciences Publishing Cor.

the function $M(f,p,k)$ with the Peclet number p for

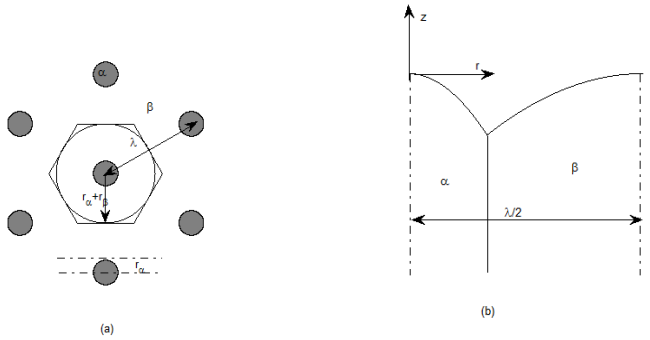

Fig 1. Schematic drawing of the rod structure. (a) Simplified geometry; (b) interface profile.

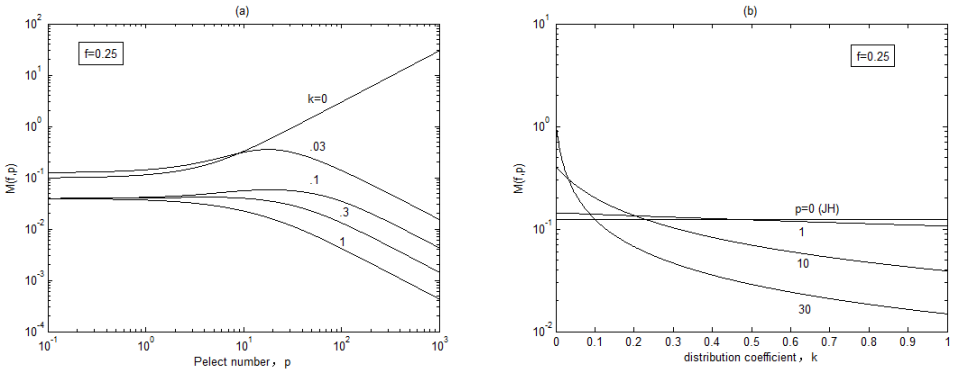

Fig 2. The variation in the function $M(f,p,k)$ for a given volume fraction $f=0.25$: (a) with the Peclet number p for different k values, and (b) with k for different Peclet number p conditions.

where $P_n = 2\gamma_n / p$, the Peclet number $p = V\lambda / 2D$, λ is the rod spacing, $\lambda = 2(r_\alpha + r_\beta)$.

The average composition at the interface in front of the α -phase $\bar{C}_\alpha$ is expressed as

$$\bar{C}_\alpha = C_\infty + A_0 + \frac{4(r_\alpha + r_\beta)V(1-k)}{D} M(f,p,k), \qquad (12)$$

where $M(f,p,k)$ is a notation

$$M(f,p,k) = \sum_{n=1}^{\infty} \frac{1}{\gamma_n^3} \frac{J_1^2(\gamma_n\sqrt{f})}{J_0^2(\gamma_n)} \frac{P_n}{\sqrt{1+P_n^2}-1+2k}, \qquad (13)$$

Similarly, the average composition at the interface in front of the β -phase $\bar{C}_\beta$ is expressed as

$$\bar{C}_\beta = C_\infty + A_0 - \frac{4r_\alpha^2(r_\alpha + r_\beta)V(1-k)}{[(r_\alpha + r_\beta)^2 - r_\alpha^2]D} M(f,p,k), \qquad (14)$$

For a fixed volume fraction, $f = 0.25$, the variations of

Different values of k , and with k for different Peclet number p are showed in **Figs.** 2(a) and 2(b), respectively. Note that there is a significant difference between large k and small k in the function $M(f,p,k)$ from **Figs**. 2. When with small Peclet number, the function $M(f,p,k)$ is a constant for each given k value. It increases rapidly with p when $k=0$, but increases slowly when k is increased, and it decreases with p when k increases further.

The stability of the interface depends not only on its temperature but also on the difference between the local actual temperature of the interface T_I and the eutectic temperature T_E . Generally, the difference between T_I and T_E consists of three parts: the solute undercooling ΔT_C , the curvature undercooling ΔT_σ and the kinetic undercooling ΔT_k . The total undercooling ΔT is expressed as

$$\Delta T = T_E - T_I = \Delta T_C + \Delta T_\sigma + \Delta T_k . \qquad (15)$$

The first part ΔT_C is generated by the departure of the local

© 2018 NSP
Natural Sciences Publishing Cor.

composition from the eutectic composition and is written as [7] $\Delta T_C = m[C_E - C(r,0)]$, where m is the slope of the liquidus. Because of non-planar interface, the second part ΔT_σ is written as [7] $\Delta T_\sigma = a^L / c(r)$, where $a^L = \Gamma \sin\theta$, a constant given by the Gibbs-Thomson relationship, and $c(r)$ is the local curvature of the interface. The third part due to the kinetic term is ΔT_k. This term depends on the chemical potential difference that drives the freezing process. And ΔT_k is written as [14] $\Delta T_k = V/\mu$, where μ is the kinetic coefficient of the eutectic phase.

Different from JH's treatment, ΔT_k cannot be ignored under rapid solidification conditions [12]. The average undercooling at the interface for the rod eutectic is obtained by substituting Eq. (12) and Eq. (14) into Eq. (15)

$$\Delta T_\alpha = m_\alpha[-C_E + C_\infty + A_0 + \frac{4V(r_\alpha + r_\beta)(1-k)}{D} M(f,p,k)] + \frac{2a_\alpha^L}{r_\alpha} + \frac{V}{\mu_\alpha}, \tag{16}$$

$$\Delta T_\beta = m_\beta[C_E - C_\infty - A_0 + \frac{4r_\alpha^2 V(r_\alpha + r_\beta)(1-k)}{[(r_\alpha + r_\beta)^2 - r_\alpha^2]D} M(f,p,k)] + \frac{2a_\beta^L r_\alpha}{(r_\alpha + r_\beta)^2 - r_\alpha^2} + \frac{V}{\mu_\beta} \tag{17}$$

Owing to the thermal diffusion in the liquid, the temperatures of the two eutectic phases at the interface are the same. Thus, Eqs. (16) and (17) can be combined to eliminate $A_0 + C_\infty$. The resultant equation, which only contains the variables λ, V, μ and ΔT, is written as

$$\frac{\Delta T}{m} = \frac{V\lambda}{D} M(f,p,k) Q_0^L + \frac{a^L}{\lambda} + \frac{V}{\mu}, \tag{18}$$

where

$$\frac{1}{m} = \frac{1}{m_\alpha} + \frac{1}{m_\beta}, \quad Q_0^L = \frac{2(1-k)}{1-f}, \tag{19}$$

$$a^L = 4\sqrt{f}\left[\frac{a_\alpha^L}{f m_\alpha} + \frac{a_\beta^L}{(1-f)m_\beta}\right], \quad \frac{1}{\mu} = \frac{1}{m_\alpha \mu_\alpha} + \frac{1}{m_\beta \mu_\beta}. \tag{20}$$

For a certain ΔT, Eq. (18) gives a series of V and λ, which is contrary to the experimental results where only one set of V and λ corresponds to a certain ΔT. Thus, an extra condition is needed to determine these two parameters. The simplest condition in which the solid was assumed to be growing at the minimum undercooling is proposed by Zener [15], and adopted by Tiller [16] and Hillert [17]. Differentiating Eq. (18), and setting $\partial(\Delta T/m)/\partial\lambda = 0$ leads to the relationship

$$V\lambda^2 = \frac{a^L}{Q_0^L / D(M + \lambda \partial M/\partial\lambda)}. \tag{21}$$

Since M is a function of the rod spacing λ, the magnitude of the small bracket is not a constant and given by

$$M + \lambda\frac{\partial M}{\partial\lambda} = \sum_{n=1}^{\infty} \frac{1}{\gamma_n^3} \frac{J_1^2(\sqrt{f}\gamma_n)}{J_0^2(\gamma_n)} \left(\frac{P_n}{\sqrt{1+P_n^2} - 1 + 2k}\right)^2 \frac{P_n}{\sqrt{1+P_n^2}}, \tag{22}$$

The minimum undercooling at the rod eutectic interface is obtained as

$$\lambda\Delta T = m a^L \left(1 + \frac{M}{M + \lambda \partial M/\partial\lambda}\right) + \frac{mV\lambda}{\mu}. \tag{23}$$

2.2 The Second Type: Cigar-Shaped Phase Diagram

For the cigar-shaped phase diagram, the difference between solute concentrations in liquid and that in solid at the α-phase interface is a constant. At the β-phase interface, it is the same, but the difference is another constant. The solute conservation condition is expressed as

$$\frac{\partial C}{\partial z}\Big|_{z=0} = -\frac{V}{D}\Delta C_\alpha, \quad 0 \le r < r_\alpha, \tag{24}$$

$$\frac{\partial C}{\partial z}\Big|_{z=0} = \frac{V}{D}\Delta C_\beta, \quad r_\alpha < r \le r_\alpha + r_\beta, \tag{25}$$

where ΔC_α and ΔC_β are two constants.

Combine the form solution of solute concentration given by Eq. (8) and the boundary condition given by (24)-(25), we obtain the Bessel coefficients A_0 and A_n

$$A_0 = fC_0 - \Delta C_\beta,$$
$$A_n = \frac{2r_\alpha V}{(r_\alpha + r_\beta)D} \frac{\gamma_n}{w_n} \frac{J_1(\gamma_n\sqrt{f})}{(J_0(\gamma_n)\gamma_n)^2} C_0, \quad n \ge 1 \tag{26}$$

where $C_0 = \Delta C_\alpha + \Delta C_\beta$.

From these results, we calculate the average concentration and the undercooling at the interface. Since the processes to obtain the results are similar to the above, for the sake of brevity, we ignore the details and give the final results directly. The average concentrations at the interface are expressed as

$$\bar{C}_\alpha = C_\infty + A_0 + \frac{4(r_\alpha + r_\beta)V}{D} C_0 M(f,p), \tag{27a}$$

$$\bar{C}_\beta = C_\infty + A_0 - \frac{4r_\alpha^2(r_\alpha + r_\beta)V}{[(r_\alpha + r_\beta)^2 - r_\alpha^2]D} C_0 M(f,p), \tag{27b}$$

where

© 2018 NSP
Natural Sciences Publishing Cor.

$$M(f,p)=\sum_{n=1}^{\infty}\frac{1}{\gamma_n^3}\frac{J_1^2(\gamma_n\sqrt{f})}{J_0^2(\gamma_n)}\frac{P_n}{1+\sqrt{1+P_n^2}}. \quad (28)$$

The undercooling at the interface is expressed as

$$\Delta T=\frac{ma^L}{\lambda}[1+\frac{M}{M+\lambda\partial M/\partial\lambda}+\frac{1}{\mu Q_0^L/D(M+\lambda\partial M/\partial\lambda)\lambda}], \quad (29)$$

where the magnitude of the small bracket is also not a constant and given by

$$M+\lambda\frac{\partial M}{\partial\lambda}=\sum_{n=1}^{\infty}\frac{1}{\gamma_n^3}\frac{J_1^2(\sqrt{f}\gamma_n)}{J_0^2(\gamma_n)}(\frac{P_n}{1+\sqrt{1+P_n^2}})^2\frac{P_n}{\sqrt{1+P_n^2}}. \quad (30)$$

And the effective kinetic undercooling

$$\Delta T_k=\frac{ma^L}{\mu Q_0^L/D(M+\lambda\partial M/\partial\lambda)\lambda^2}. \quad (31)$$

3 Discussions

3.1 The Effects of Peclet Number p and Distribution Coefficient k on the Rod Eutectic Growth

When the kinetic parameter is very large, the kinetic term is ignored. Combining Eq. (23) with Eq. (30) and letting $\mu\to\infty$, we derive

$$\Delta T=2mQ_0^L p(2M+\lambda\partial M/\partial\lambda). \quad (32)$$

For simplification, we define reasonable dimensionless parameters:

$$\bar{\lambda}=\frac{\lambda C_0}{\sqrt{f}[(1-f)a_\alpha^L/f\,m_\alpha+a_\beta^L/m_\beta)]},\ \Delta\bar{T}=\frac{\Delta T}{2mC_0}.$$

In terms of these dimensionless parameters, the results is written as

$$\bar{\lambda}=\frac{1}{p}(M+\lambda\partial M/\partial\lambda)\quad,\quad\Delta\bar{T}=\frac{2p}{1-f}(2M+\lambda\partial M/\partial\lambda)\quad. \quad (33)$$

Compared with the model of JH [7], the results suggest that the rod eutectic growth is affected by Peclet number p and distribution coefficient k. We show the variations of $\bar{\lambda}$ and $\Delta\bar{T}$ versus the variable p in **Figs.** 3 and 4, for the first type phase diagram and the second type phase diagram, respectively. We can see that both the rod spacing and the interface undercooling changes differently compared with the results obtained by the JH when the Peclet number is larger than one. **Fig**. 3(a) and **Fig**. 4(a) shows the variation of the rod spacing versus the Peclet number. For the first type phase diagram as see in **Fig**. 3(a), $\bar{\lambda}$ decreases continuously, but the slope changes near $p=1$. For the second type phase diagram as see in **Fig**. 4(a), $\bar{\lambda}$ initially decreases, then increases with the increase of the Peclet number. Similarly, for the first type phase diagram as see in **Fig**. 3(b), the $\Delta\bar{T}$ increases continuously with the Peclet number, but a change in slope is found near $p=1$, while for the second type phase diagram as see in **Fig**. 4(b) it initially increases with the increase of the Peclet number, but it approaches a constant when the Peclet number is larger than ten.

The precise manner in which the value of k effects $\bar{\lambda}$ and $\Delta\bar{T}$ can be seen in **Figs.** 5. We find that when $p\geq1$ there are significant differences both for the interface undercooling and the rod spacing. Maximum value of the interface undercooling is obtained for each distribution coefficient k except for the case $k=0$.

As we see in the **Fig.** 6, the expression λ^2V approximates to a constant for the rod eutectic with $p<1$ for a fixed value of k, which agrees well with the results proposed by Jackson and Hunt [7]. But it does not hold at high velocities. The variation in the expression λ^2V with the Peclet number shows a non-constant behavior at high velocities, as showed in **Fig.** 6.

3.2 The Effect of kinetic parameter μ on the Rod Eutectic Growth

Different from the theories of JH [7] and TMK [8], our study incorporate the interface kinetic undercooling into the total undercooling. We find that the rod eutectic growth is definitely affected by the interface kinetics. **Fig.** 7 (a) shows the variation in undercooling with the rod eutectic growth velocities. As the velocity increases, the undercooling increases continuously. Compared with the TMK (where $\mu=\infty$, it represents the crystal growth without considering kinetic effect), no obvious difference is found at $\mu=1$. But there is an obvious difference at $\mu=0.1$ and a significant difference at $\mu=0.05$. For a fixed undercooling, as the kinetic parameter increases, the rod eutectic growth velocity also increases. **Fig.** 7 (b) shows the variation in undercooling with the rod spacing. As the rod spacing increases, the undercooling decreases. Compared with the TMK, no obvious difference is seen at $\mu=1$. But there is an obvious difference at $\mu=0.1$ and a significant difference at $\mu=0.05$. The kinetic parameter increases as the rod spacing decreases for a fixed undercooling. **Fig.** 7 (c) shows the percentage of the kinetic undercooling in the total undercooling at different values of μ. We see that it could be ignored when μ is large, but should be taken into consideration when μ is small. It is

© 2018 NSP
Natural Sciences Publishing Cor.

more than ten percent when $\mu = 0.1$, and further rises up to dozens percent when $\mu = 0.05$.

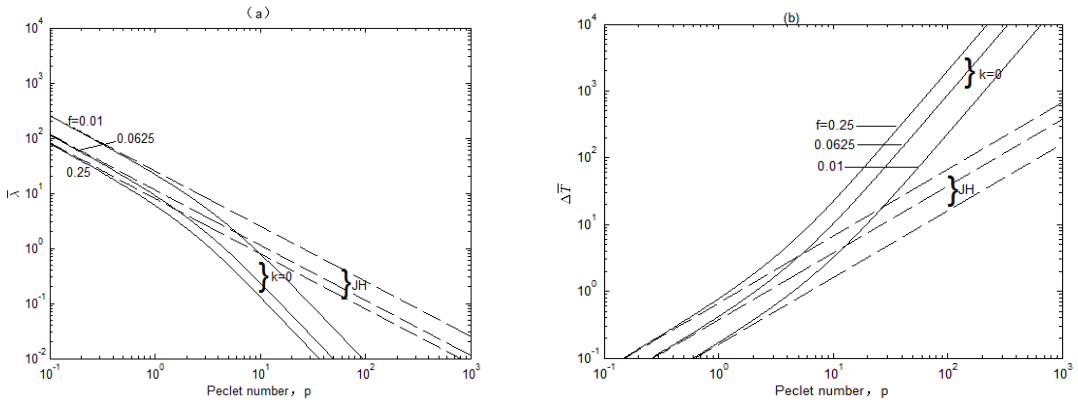

Fig. 3 Variations in (a) dimensionless rod spacing $\bar{\lambda}$ and (b) dimensionless minimum interface undercooling $\Delta\bar{T}$ with the Peclet number p for $k = 0$.

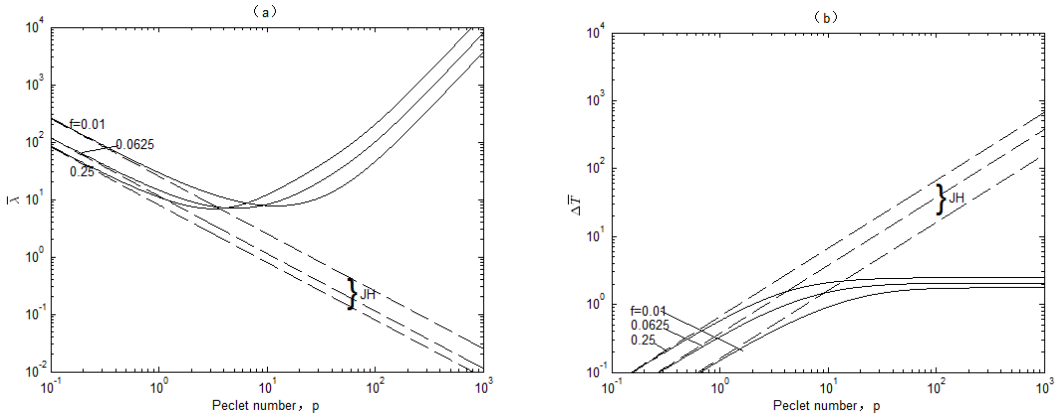

Fig. 4 Variations in (a) dimensionless rod spacing $\bar{\lambda}$ and (b) dimensionless minimum interface undercooling $\Delta\bar{T}$ with the Peclet number p for the second type phase diagram.

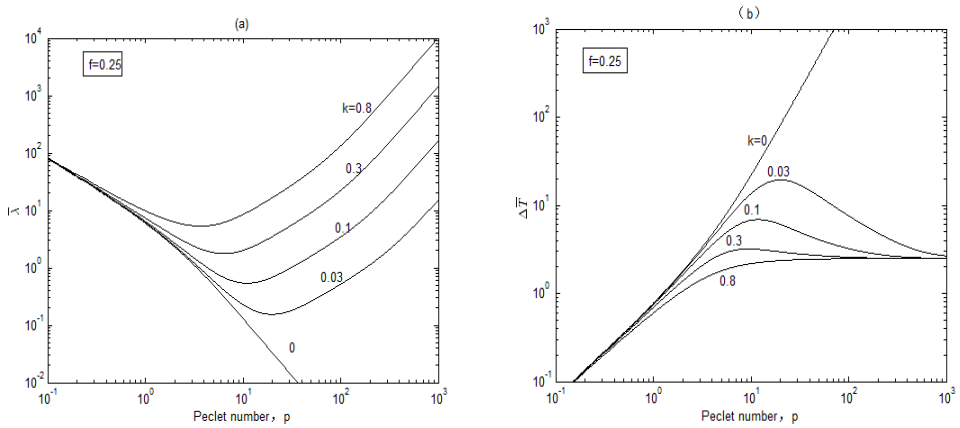

Fig. 5 The variation of (a) dimensionless rod spacing $\bar{\lambda}$ and (b) dimensionless undercooling $\Delta\bar{T}$ with Peclet number p for different values of k, when the volume fraction $f = 0.25$.

© 2018 NSP
Natural Sciences Publishing Cor.

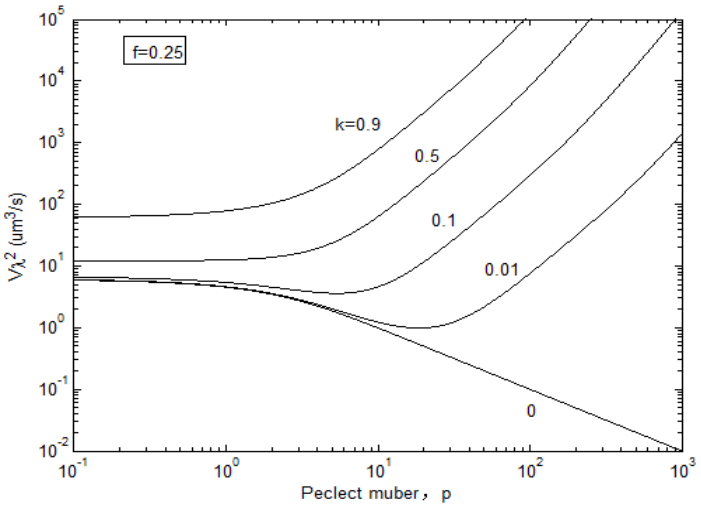

Fig. 6 The variation in expression $\lambda^2 V$ with Peclet number p .

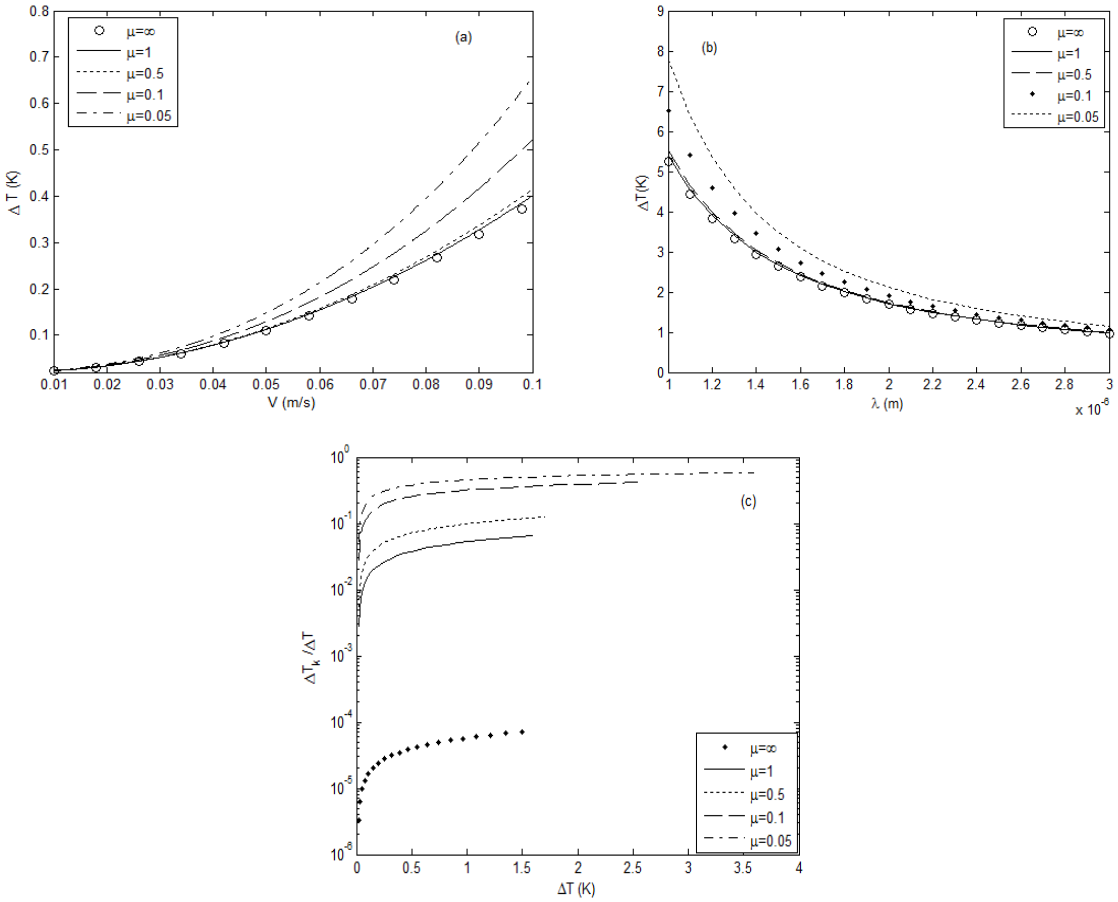

Fig. 7 The eutectic growth velocities (a) rod spacing; (b) and the percentage of kinetic under cooling in the total under cooling; (c) when $m_\alpha = m_\beta = 5\,\mathrm{K/at.\%}$, and $C_0 = 10\,\mathrm{at.\%}$.

© 2018 NSP
Natural Sciences Publishing Cor.

4 Conclusions

We extend the theory of rod eutectic growth by Jackson and Hunt from low velocities to high velocities under rapid solidification and investigate the kinetic effect on the rod eutectic growth. The results reveal that small rod spacing and a large undercooling in the system require large Peclet number p coupled with small distribution coefficient k. The effects of p and k are found to be significant under rapid solidification conditions. And these effects cause the expressions $\lambda^2 V$ and $\lambda\Delta T$, which are constants at low velocities, to become variables at high velocities. When the rod eutectic has the phases with small kinetic parameters and grows under rapid solidification conditions, the effect of interface kinetics on the rod eutectic growth is significant and the rod spacing varies with the kinetic parameters. The kinetic parameter increases as the rod spacing decreases for a fixed undercooling. The interface kinetics effect can make a contribution to the growth velocity.

Acknowledgments

The authors wish to thank Professor Zi-Dong Wang (University of Science and Technology Beijing, China) for his support and help.

Reference

[1] Pan Y and Sun G X 1996 *Acta Metall. Sin.* **32** 120 (in Chinese)

[2] Zimmermann M, Carrard M and Kurz W 1989 *Acta Metall.* **37** 3305

[3] Zhang J F, Shen J , Shang Z, Feng Z R, Wang L S and Fu H Z 2011 *J. Cryst. Growth* **329** 77

[4] Livingston J D, Cline H E, Koch E F and Russell R R 1970 *Acta Metall.* **18** 399

[5] Mergy J, Faivre G, Guthmann C and Mellet R 1993 *J. Cryst. Growth* **134** 353

[6] Ludwig A and Leibbrandt S 2004 *Mat. Sci. Eng. A* **375-377** 540

[7] Jackson K A and Hunt J D 1966 *Trans. AIME* **236** 1129

[8] Trivedi R, Magnin P and Kurz W 1987 *Acta Metall.* **35** 971

[9] Hunt J D and Jackson K A 1966 *Trans. Metall. Soc. AIME* **236** 843

[10] Li J F and Zhou Y H 2005 *Acta Mater.* **53** 2351

[11] Trivedi R and Wang N 2012 *Acta Mater.* **60** 3140

[12] Li J F and Zhou Y H 2005 *Sci. China Ser. E* **48** 361 (in Chinese)

[13] Li M, Yoda S and Kuribayashi K 2005 *Philos. Mag.* **85** 2581

[14] Herlach D M and Feuerbacher B 1991 *Adv. Space Res.* **11** 255

[15] Zener C 1946 *Trans. AIME* **167** 550

[16] Tiller W A 1958 *Liquid Metals and Solidification* (Cleceland, Ohio: American Society of Metals) p. 126

[17] Hillert M and Steinhauser H 1960 *Jemont. Ann.* **144** 520

© 2018 NSP
Natural Sciences Publishing Cor.